INTERNATIONAL JOURNAL OF NUMERICAL MODELLING: ELECTRONIC NETWORKS, DEVICES AND FIELDS
Int. J. Numer. Model. 2005; **18**:49–66
Published online 19 October 2004 in Wiley InterScience (www.interscience.wiley.com). DOI: 10.1002/jnm.561)

Efficient hybrid scheme of finite element method of lines for modelling computational electromagnetic problems

R. S. Chen[1,*,†], Edward K. N. Yung[2] and Ke Wu[3]

[1] *Department of Communication Engineering, Nanjing University of Science and Technology, Nanjing 210094, People's Republic of China*
[2] *Department of Electronic Engineering, City University of Hong Kong, Hong Kong SAR, People's Republic of China*
[3] *Department of Electrical and Computer Engineering, École Polytechnique, Montreal, Canada*

SUMMARY

A hybrid scheme called finite element method of lines is proposed and described for modelling and analysis of generalized computational electromagnetic problems with emphasis on a number of irregular waveguide examples. This new technique is developed by combining a finite element method with a method of lines so that it can handle not only irregular composite geometry but also maintain high accuracy enjoyed by semi-analytical procedures. Analytical and numerical algorithmic building blocks of this new scheme are discussed in detail such as geometry discretization, element mapping, element trial functions, reformulation and computational issues of non-linear ordinary differential equations. Our results show that this new technique is able to efficiently solve complex problems as compared with the conventional method of lines.

KEY WORDS: finite element method; method of lines; computational electromagnetics; guided-wave problems; differential equation methods; variational analysis

1. INTRODUCTION

Guided-wave and transmission line problems are the foundation for design of integrated circuits and devices at frequencies ranging from megahertz to terahertz, which have been studied by researchers for a long time. With few exceptions, the existing analytical solutions are only amenable to structures of homogeneous material and of simple regular geometry such as circular, rectangular, elliptical, annular or other co-ordinate-conformable topology, for which the method of separation of variables can be applied. As for an arbitrarily shaped transmission line, however, the solution is obtainable only numerically, for example, the finite difference

*Correspondence to: Prof R. S. Chen, Department of Communication Engineering, Nanjing University of Science and Technology, Nanjing 210094, People's Republic of China.
† E-mail: eerschen@mail.njust.edu.cn

Conract/grant sponsor: Natural Science Foundation of China; contract/grant numbers: 60271005, 60371002
Contract/grant sponsor: Excellent Youth Natural Science Foundation of China; contract/grant number: 60325103

Received April 2002
Revised June 2004
Accepted August 2004

method, the finite element method (FEM) as well as the boundary equation method. In particular, the FEM has become a very popular tool in solving electromagnetic problems because it is able to handle with great flexibility a large class of geometrically and compositionally complex problems [1–3]. Nevertheless, the FEM has to fully discretize a problem into a system of algebraic equations with discrete nodal/edge potential or field values as basic unknowns and thus errors of discretization are inevitably introduced. Mesh density must be small enough to obtain accurate solutions and locally adaptive mesh refinement is necessary when there is a singularity in the computational domain.

It is, of course, desirable to solve boundary-value problems in an analytical manner whenever possible. The method of lines (MOL) is a semi-discrete and semi-analytical method and it has found applications in simulating and modelling multi-layer planar circuits [4–8]. However, the conventional MOL makes use of a finite difference technique to discretize the problem and turn it into a set of analytically solvable ordinary differential equations (ODEs) with nodal line functions as the basic unknowns. Different from the conventional MOL, our proposed hybrid finite element method of lines FEMOL scheme utilizes a finite element technique in a semi-discrete form [9–14]. Partial differential equations (PDEs) defined on some particular domains even though they may be arbitrary are semi-discretized into a system of ODEs defined on discrete mesh lines (straight or curved) via variational principles, and then the resulting ODE system can directly be solved using a standard and robust ODE solver. Due to the efficient adaptivity and the so-called super-convergence capability built into today's ODE solvers, highly reliable and accurate solutions of the ODE system can be obtained numerically, and hence the semi-analytical characteristics featured in this method are well preserved.

As a semi-analytical or semi-discrete method, the FEMOL makes itself distinguished from the standard FEM procedures in view of several aspects. Intuitively, this method should be powerful and efficient, in particular, for those field problems for which solutions, for example in a two-dimensional (2D) case, may exhibit quite 'wild' behaviour in one direction and rather 'mild' in the other. For the standard line meshes, both FEMOL and FEM share the same convergence order in the formulated energy norms. But the errors in a FEMOL solution are independent of the true solution variation in the mesh line direction. In other words, no matter how naughty the true solution behaves along the mesh line direction, we will be able to gain an equally or consistently accurate FEMOL solution as long as the behaviours of the true solutions are similar to that of the FEM along the discrete direction. This characteristic is very attractive when there is a singularity in the computational domain. On the other hand, the use of robust ODE solvers makes the solution of the resulting ODEs (generally with variable coefficients) unified, efficient, accurate and effortless as compared with the conventional MOL in which a linear transformation is required to de-couple the coupled ODEs.

In this paper, basic concepts and analytical formulations of the proposed FEMOL hybrid algorithm are detailed by solving an elliptic Helmholtz equation boundary value problem. In Section 2, algorithmic properties and procedures of geometry discretization, element mapping and element trial functions in the FEMOL are discussed in depth. In Section 3, several numerical examples are given to showcase the accuracy and efficiency of this new numerical technique through modelling and analysis of waveguide eigen-value problems.

2. THEORY AND FORMULATION

To begin with, let us consider a problem of the elliptic model, for example, Helmholtz equation,

$$\nabla^2 u + \lambda u = 0 \quad \text{over } \Omega \tag{1}$$

$$u = \bar{u}(x, y) \quad \text{on } \Gamma_D \tag{2}$$

$$\frac{\partial u}{\partial n} = g \quad \text{on } \Gamma_N \tag{3}$$

where the 2D domain Ω is bounded by a segmented boundary with differential element $\partial\Omega$ that consists of Dirichlet boundary Γ_D and Neumann boundary Γ_N, for example, $\partial\Omega = \Gamma_D \cup \Gamma_N$, and n denotes the outward normal orientation. For the problem defined above, it can be shown that its solution can be obtained by solving the equivalent variation problem defined by

$$\begin{cases} \delta F(u) = 0 \\ u|_{\Gamma_D} = \bar{u}(x, y) \end{cases} \tag{4}$$

where

$$F(u) = \frac{1}{2} \iint_{\Omega} \left[\left(\frac{\partial u}{\partial x} \right)^2 + \left(\frac{\partial u}{\partial y} \right)^2 + \lambda u^2 \right] \mathrm{d}A - \int_{\Gamma_n} gu \, \mathrm{d}\Gamma$$

in which u satisfies the essential boundary conditions (2). It is readily proved that searching for a solution of the PDE problem (1) is equivalent to finding a u that minimizes the functional equation (4). There are a number of ways to do so; our interest is to develop a new scheme called FEMOL, which can effectively be applied herewith. This new technique will be described in detail in the subsequent sections.

2.1. Domain discretization and parametric element mapping

To explain our proposed FEMOL, first of all, we segment the domain Ω into N quadrilateral elements e_k $(k = 1, 2, \ldots, N)$ so that $\Omega = \Omega_h = \bigcup_{k=1}^{N} e_k$ depending on whether Ω_h covers Ω exactly or not. To simplify our mathematical description, the subscript k is dropped off when referring to a representative element unless otherwise specified. Geometrical shapes of the elements depend on mapping functions of the elements. However, all the four edges of an element are generally allowed to be in the curved form, leading to a convenient and flexible modelling of irregular or arbitrary domains.

As an example, Figure 1 shows a possible FEMOL mesh arrangement for an irregular 2D domain, in which $\{1\}, \{2\}, \ldots,$ denote the global mesh line number and $1, 2, \ldots,$ denote the global end-node number. The dashed lines in quadratic elements stand for the internal mesh lines. Figure 2(a) shows a typical quadratic element mapping in the FEMOL from a local (ξ, η) space to the global (x, y) space. The curves are defined by $\xi = \xi_i = -1 + 2(i-1)/\hat{p}$, $i = 1, 2, \ldots, \hat{p} + 1$, which are called element nodal lines and the ith nodal line is denoted, for example, by L_i. The two boundary curves are defined by $\eta = \eta_i = -1 + 2(j-1)$, $j = 1, 2$, which are called element end-sides, and the jth end-side is denoted, for example, by S_j. The intersections of L_i and S_j are defined by $(\xi_i, \eta_j) = L_i \cap S_j$, $i = 1, 2, \ldots, \hat{p} + 1$, $j = 1, 2$, which are called node ij of an element with symbol η_{ij}. The element mapping is set up in two steps, namely, the nodal line mapping and the interpolation to the nodal lines.

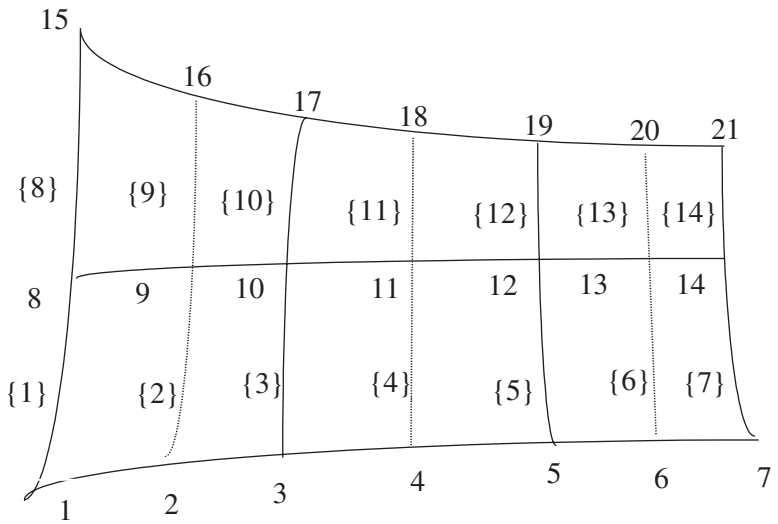

Figure 1. Descriptive mesh or segmentation arrangement of the proposed FEMOL for arbitrary computational domain with boundary conditions.

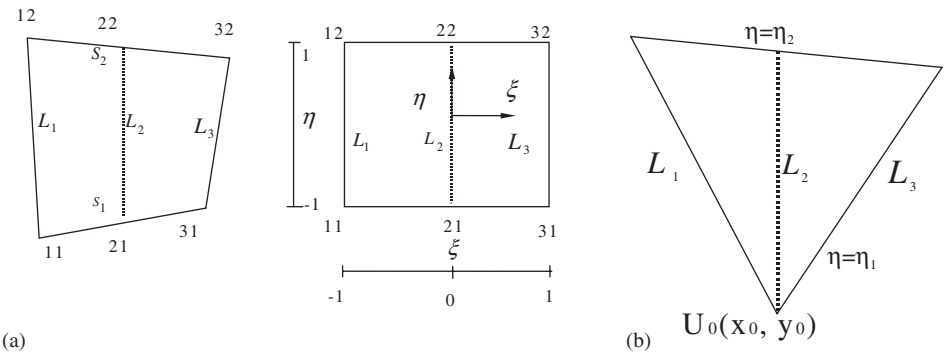

Figure 2. (a) A quadratic element mapping between the global space and local space; and (b) An element with a degenerate end-side.

The first step is to map the curved nodal lines in (x, y) space to a standard straight-line segment η from -1 to $+1$ so that a typical nodal line L_i is formulated in a parametric manner as

$$x = x_i(\eta), \quad y = y_i(\eta), \quad -1 \leqslant \eta \leqslant +1 \tag{5}$$

Although the exact curve mapping is analytically possible in some cases, approximate mappings are much preferred for the purpose of a computational flexibility and versatility. The domain partition has been discussed in detail in References [9–13]. However, quadrilaterial elements do not provide enough convenient modelling of irregular or arbitrary domains and then triangular elements are introduced in this section to enhance the flexibility and versatility of this hybrid method. The triangular element may be regarded as an element with an end-side S_j degenerating to point. In this case the Jacobin determinant J of the triangular element vanishes at the

degenerated point and hence singularity arises in the formulation in References [10–13] involving that end-side if the generated point is a Neumann point or an interior point.

Consider an element e and let one of its end-side $\hat{S}_j$ degenerate to a point (x_0, y_0) as shown in Figure 2(b). For the ith nodal line curve defined by $(x_i(\eta), y_i(\eta))$, by expanding $x_i(\eta)$ and $y_i(\eta)$ into the Taylor series about point $\eta = \eta_j$ we obtain

$$x_i(\eta) = x_0 + (\eta - \eta_j)x_i'(\eta_j) + (\eta - \eta_j)^2 x_i''(\eta_j)/2 + \cdots \tag{6a}$$

$$y_i(\eta) = y_0 + (\eta - \eta_j)y_i'(\eta_j) + (\eta - \eta_j)^2 y_i''(\eta_j)/2 + \cdots \tag{6b}$$

The manner to remove singularities is to decompose each vanishing term at $\eta = \eta_j$ into a product of a linear vanishing factor $(\eta - \eta_j)$ and a non-vanishing term, so that the vanishing factor $(\eta - \eta_j)$ can be completely cancelled in the subsequent asymptonic analysis. Therefore, the above equations can be rewritten in the following compact form:

$$\begin{Bmatrix} x_i(\eta) \\ y_i(\eta) \end{Bmatrix} = \begin{Bmatrix} x_0 \\ y_0 \end{Bmatrix} + (\eta - \eta_j)\begin{Bmatrix} \hat{x}_i(\eta) \\ \hat{y}_i(\eta) \end{Bmatrix} \tag{7}$$

As the nodal line mapping is completed, the element mapping is readily made by the use of a Lagrange interpolation in ξ direction in the local space, such as

$$\begin{Bmatrix} x \\ y \end{Bmatrix} = \begin{Bmatrix} x_0 \\ y_0 \end{Bmatrix} + (\eta - \eta_0)\sum_{i=1}^{\hat{p}+1} N_i(\xi)\begin{Bmatrix} \hat{x}_i(\eta) \\ \hat{y}_i(\eta) \end{Bmatrix} \tag{8}$$

Subsequently, we have

$$\begin{Bmatrix} \dfrac{\partial}{\partial \xi} \\ \dfrac{\partial}{\partial \eta} \end{Bmatrix} = [J]\begin{Bmatrix} \dfrac{\partial}{\partial x} \\ \dfrac{\partial}{\partial y} \end{Bmatrix}, \quad \begin{Bmatrix} \dfrac{\partial}{\partial x} \\ \dfrac{\partial}{\partial y} \end{Bmatrix} = [J]^{-1}\begin{Bmatrix} \dfrac{\partial}{\partial \xi} \\ \dfrac{\partial}{\partial \eta} \end{Bmatrix} \tag{9}$$

in which the Jacobian matrix $[J]$ of the co-ordinate transformation and its inversion can easily be obtained by the following explicit equations:

$$[J] = (\eta - \eta_j)[\hat{J}], \quad [J]^{-1} = \frac{1}{\hat{J}}\begin{bmatrix} y_\eta/(\eta - \eta_j) & -\hat{y}_\xi \\ -x_\eta/(\eta - \eta_j) & \hat{x}_\xi \end{bmatrix} \tag{10}$$

where

$$[\hat{J}] = \begin{bmatrix} \hat{x}_\xi & \hat{y}_\xi \\ x_\eta & y_\eta \end{bmatrix}$$

and $\hat{x}_\xi = \partial x_\xi/\partial\eta$, $\hat{y}_\xi = \partial y_\xi/\partial\eta$ at $\eta = \eta_j$. Note that $|J|$ vanishes at $\eta = \eta_j$ but $|\hat{J}|$ does not. Furthermore, the singularity in the first column of $[J]^{-1}$ will be removed when it is practically applied to calculation of partial derivatives.

2.2. *Energy functional in triangular element*

The trial function u over triangular element e may be approximated by a certain shape function in ξ direction, and it remains continuous and unknown in η direction. A convenient choice for

the shape function is the Lagrange interpolating polynomials of degree p as follows:

$$u = \sum_{i=1}^{p+1} N_i(\xi)\Phi_i(\eta) \quad -1 \leqslant \xi, \ \ \eta \leqslant 1 \tag{11}$$

where

$p = 1$

$$N_1(\xi) = \tfrac{1}{2}(1-\xi), \quad N_2(\xi) = \tfrac{1}{2}(1+\xi)$$

$p = 2$

$$N_1(\xi) = \tfrac{1}{2}(\xi^2 - \xi), \quad N_2(\xi) = 1 - \xi^2, \quad N_3 = \tfrac{1}{2}(\xi^2 + \xi)$$

$p = 3$

$$N_1(\xi) = \tfrac{1}{16}(1-\xi)(9\xi^2 - 1), \quad N_2(\xi) = \tfrac{9}{16}(\xi^2 - 1)(3\xi - 1)$$

$$N_3(\xi) = -\tfrac{9}{16}(\xi^2 - 1)(3\xi + 1), \quad N_4(\xi) = \tfrac{1}{16}(1+\xi)(9\xi^2 - 1)$$

The nodal line functions follow the same rule as in Equation (7), i.e.

$$\Phi_i(\eta) = u_0 + (\eta - \eta_j)\hat{\Phi}_i(\eta) \tag{12}$$

where u_0 is the function value at the degenerated point. Substituting (12) into (11) we obtain

$$u = u_0 + (\eta - \eta_j)\sum_{i=1}^{p+1} N_i(\xi)\hat{\Phi}_i(\eta) \tag{13}$$

It should be pointed out that the elements defined in Figure 2 are used for geometry modelling and the trial functions pertaining to such elements may take different approximate functions. Substituting (13) into (5), the energy functional for triangular element e can be written in general by

$$F(\{\Phi\}^e) = \int_\Omega L\left(\eta, \{\Phi\}^e, \frac{\partial\{\Phi\}^e}{\partial\eta}\right) \mathrm{d}\Omega$$

and in detail as follows:

$$F(\{\Phi\}^e) = \frac{1}{2}\int_{-1}^{1} (\{\Phi'\}^{e\mathrm{T}}[A]^e\{\Phi'\}^e + 2\{\Phi'\}^{e\mathrm{T}}[B]^e\{\Phi\}^e + \{\Phi\}^{e\mathrm{T}}[C]^e\{\Phi\}^e + \lambda\{\Phi\}^{e\mathrm{T}}[M]^e\{\Phi\}^e)\,\mathrm{d}\eta$$
$$- \int_{-1}^{1} \{\Phi\}^{e\mathrm{T}}\{F\}^e\,\mathrm{d}\eta - \sum_{j=1}^{2} \{\Phi(\eta_j)\}^{e\mathrm{T}}\{P_j\}^e \tag{14}$$

where

$$[A]^e = (\eta - \eta_j)[\hat{A}]^e, \quad [\hat{A}]^e = \int_{-1}^{1} a(\xi,\eta)[N]^{\mathrm{T}}[N]\,\mathrm{d}\xi, \quad a(\xi,\eta) = [(\hat{x}_\xi)^2 + (\hat{y}_\xi)^2]/\hat{J}$$

$$[B]^e = [\hat{B}]^e, \quad [\hat{B}]^e = \int_{-1}^{1} b(\xi,\eta)[N]^{\mathrm{T}}[N']\,\mathrm{d}\xi, \quad b(\xi,\eta) = -(\hat{x}_\xi x_\eta + \hat{y}_\xi y_\eta)/\hat{J}$$

$$[C]^e = (\eta - \eta_j)^{-1}[\hat{C}]^e, \quad [\hat{C}]^e = \int_{-1}^{1} c(\xi,\eta)[N']^{\mathrm{T}}[N']\,\mathrm{d}\xi, \quad c(\xi,\eta) = [(x_\eta)^2 + (y_\eta)^2]/\hat{J}$$

$$[M]^e = (\eta - \eta_j)[\hat{M}]^e, \quad [\hat{M}]^e = \int_{-1}^{1} [N]^{\mathrm{T}}[N]\hat{\boldsymbol{J}}\,\mathrm{d}\xi$$

$$\{F\}^e = \{J_{L_1} g_{L_1}, 0, \ldots, 0, J_{L_{p+1}} g_{L_{p+1}}\}, \quad g_{L_i} = g(L_i)$$

$$\{P_j\}^e = \int_{-1}^{1} \{\Phi\}^{\mathrm{T}} g_{S_j} J_{S_j}\,\mathrm{d}\xi, \quad g_{S_j} = g(S_j)$$

2.3. Variational equation in FEMOL

Once energy functional in triangular/quadrilateral element is expressed, the variation principle is used to derive the first variation of the element functional. Since the operation of variation is cumulative with respect to both integration and differentiation, the first variation of F due to an incremental change in solution Φ can be expressed as

$$\begin{aligned} \partial F &= \int_\Omega \left(\frac{\partial L}{\partial \Phi}\delta\Phi + \frac{\partial L}{\partial \Phi_\eta}\delta\Phi_\eta \right) \mathrm{d}\Omega \\ &= \int_\Omega \left(\frac{\partial L}{\partial \Phi}\delta\Phi + \frac{\partial L}{\partial \Phi_\eta}\frac{\partial}{\partial \eta}\delta\Phi \right) \mathrm{d}\Omega \end{aligned} \tag{15}$$

in which $\Phi_\eta = \partial\Phi/\partial\eta$ and $\delta\Phi_\eta = \delta\partial\Phi/\partial\eta = \partial\delta\Phi/\partial\eta$. Integrating the second term by parts and applying Green–Gauss theorem yields

$$\begin{aligned} \int_\Omega \frac{\partial L}{\partial \Phi_\eta}\frac{\partial(\delta\Phi)}{\partial\eta}\mathrm{d}\Omega &= \int_\Omega \frac{\partial}{\partial\eta}\left(\frac{\partial L}{\partial \Phi_\eta}\delta\Phi\right)\mathrm{d}\Omega - \int_\Omega \frac{\partial}{\partial\eta}\left(\frac{\partial L}{\partial \Phi_\eta}\right)\delta\Phi\,\mathrm{d}\Omega \\ &= \int_\Gamma l_\eta \frac{\partial L}{\partial \Phi_\eta}\delta\Phi\,\mathrm{d}\Omega - \int_\Omega \frac{\partial}{\partial\eta}\left(\frac{\partial L}{\partial \Phi_\eta}\right)\delta\Phi\,\mathrm{d}\Omega \end{aligned} \tag{16}$$

in which l_η is the direction cosine of the normal to the outer surface with respect to the η axis. And then ∂F can be expressed as

$$\partial F = \int_\Omega \left[\frac{\partial L}{\partial \Phi} - \frac{\partial}{\partial\eta}\frac{\partial L}{\partial \Phi_\eta}\right]\delta\Phi\,\mathrm{d}\Omega + \int_\Gamma \frac{\partial L}{\partial \Phi_\eta} l_\eta \delta\Phi\,\mathrm{d}\Gamma \tag{17}$$

Substituting Equations (11) and (12) into Equation (15), the first-order differentiation of the element functional with integration by parts yields

$$\begin{aligned} \partial F^e(\{\Phi\}^e) = &- \int_{-1}^{1} \{\partial\Phi\}^{e\mathrm{T}}([A]^e\{\Phi''\}^e + [G]^e\{\Phi'\}^e + [H]^e\{\Phi\}^e + \lambda[M]^e\{\Phi\}^e)\,\mathrm{d}\eta \\ &+ \sum_{j=1}^{2} \eta_j \{\partial\Phi(\eta_j)\}^{e\mathrm{T}}(\{Q_j\}^e - \eta_j\{P_j\}^e) \end{aligned} \tag{18}$$

where

$$[G]^e = [A']^e + [B]^e - [B]^{e\mathrm{T}}, \quad [H]^e = [B']^e - [C]^e$$

$$\{Q_j\}^e = [A]^e\{\Phi'\}^e + [B]^e\{\Phi\}^e, \quad \eta = \eta_{\mathrm{j}};\ j = 1, 2$$

$$[A']^e = \int_{-1}^{1} \frac{\partial a(\xi,\eta)}{\partial \eta}[N]^{\mathrm{T}}[N]\,\mathrm{d}\xi, \quad [B']^e = \int_{-1}^{1} \frac{\partial b(\xi,\eta)}{\partial \eta}[N]^{\mathrm{T}}[N']\,\mathrm{d}\xi$$

The trial functions are required to be globally continuous and also satisfy essential boundary conditions. The continuity condition across common nodal lines can be realized in the element assembling procedure in a similar fashion to that of the FEM.

2.4. Ordinary differential equation (ODE) system for the FEMOL

Now, the resulting ODE system from the FEMOL approximation to the Helmholtz problem (1) can be summarized as follows:

$$[A]\{\Phi''\} + [G]\{\Phi'\} + [H]\{\Phi\} + \lambda[M]\{\Phi\} = \{0\}, \quad -1 < \eta < 1 \tag{19}$$

This is the derived set of a second-order ODE system to be solved in conjunction with the boundary conditions at end-points of the nodal lines. Obviously, the boundary conditions and related aspects should be examined. Let us consider a typical component Φ_m in $\{\Phi\}$, which represents mth line function value at jth end node ($j = 1, 2$). This end node could also be an internal common node with another line n , such as nodes 9, 10 and 11 as described in Figure 1. We can then distinguish three different cases by

(a) *Dirichlet node*: This end node is on Γ_D and Equation (14) will be satisfied ($\partial\Phi_m = 0$) if we simply interpolate the data generated by imposing $\Phi_m = \bar{\Phi}_m$ and $\eta = \eta_j$, $j = 1, 2$.
(b) *Neumann node*: This end node is on Γ_N and hence $\partial\Phi_m$ is arbitrary, yielding $Q_{jm} = \eta_j P_{jm}$, $\eta = \eta_j$, $j = 1$ or 2.
(c) *Interface node*: This end node of mth line is an internal interface node shared with line n, and hence $\partial\Phi_m$ is arbitrary but subject to a constraint given by $\partial\Phi_m = \partial\Phi_n$, leading to $\Phi_m = \Phi_n$, and $Q_{jm} + Q_{jn} = 0$, $\eta = \eta_j$, $j = 1$ or 2.

Such second-order ODE systems can be solved with some currently available ODE solvers together with boundary conditions [15–17]. To formulate relevant matrices and vectors in the above ODE systems, a definite integration in ξ direction is required by using a Gaussian numerical integration. It can be observed from the above equations that the proposed FEMOL makes the approximation by a set of ODE systems, which is different from the FEM that makes the approximation leading to a PDE by a set of algebraic equations. The FEMOL, in light of its algorithmic platform between the FEM and analytical techniques, gets a step closer to the original field problem judging from the degree of discretization, the equation characteristics, and expected solution accuracy.

2.5. Equation reformulation and algorithm development

For the sake of readability, the above ODE system (19) is arranged into the following general ODE matrix form:

$$[L]\{\Phi(\eta)\} = \lambda[M]\{\Phi(\eta)\}, \quad -1 \leqslant \eta \leqslant 1 \tag{20}$$

which is also subject to the boundary conditions $[B_{-1}]\{\Phi(-1)\} = \{0\}, [B_1]\{\Phi(1)\} = \{0\}$. λ stands for eigen-value of the ODE systems, $\{\Phi\}$ is a related n-vector eigen-function of η, and $[L]$, $[M]$, $[B_{-1}]$, as well as $[B_1]$ are ordinary differential linear operator matrices with such usual properties

as self-adjoint, positive, non-singular, and so forth. When the Rayleigh quotient is applied to calculate the eigen-value of (20), we have $\lambda = \int_{-1}^{1} \{\Phi\}^{\mathrm{T}}[L]\{\Phi\}\,\mathrm{d}\eta / \int_{-1}^{1} \{\Phi\}^{\mathrm{T}}[M]\{\Phi\}\,\mathrm{d}\eta$.

Although the currently available ODE solvers are powerful enough for standard linear and non-linear ODE systems, most of them are not furnished with eigen-solution features and thus the eigen- problems related to the ODE systems are not in a form solvable by a standard ODE solver. Nevertheless, they can easily be transformed into acceptable forms by adding only two first-order differential equations as developed by Ascher and Russell [18] and Quanfeng [19].

First of all, we introduce a trial ODE for the eigen-value

$$\lambda' = 0 \tag{21}$$

which guarantees λ to be a constant. To achieve solution uniqueness for the eigen-function $\{\Phi\}$, a condition of normalization is applied, and it can be formulated as $\|\Phi\|_M^2 = \frac{1}{2}\int_{-1}^{1} \{\Phi\}^{\mathrm{T}}[M]\{\Phi\}\,\mathrm{d}\eta = 1$. This condition may also be converted into an equivalent ODE form as follows:

$$R' = \tfrac{1}{2}\{\Phi\}^{\mathrm{T}}[M]\{\Phi\}, \quad -1 \leqslant \eta \leqslant 1$$

$$R(-1) = 0, \quad R(1) = 1 \tag{22}$$

Then (20)–(22) constitute a standard non-linear system of ODE as

$$\lambda' = 0$$

$$R' = \{\Phi\}^{\mathrm{T}}[M]\{\Phi\}$$

$$[A]\{\Phi''\} + [G]\{\Phi'\} + [H]\{\Phi\} + \lambda[M]\{\Phi\} = \{0\}, \quad -1 \leqslant \eta \leqslant 1 \tag{23}$$

with the boundary conditions

$$R(-1) = 0, \quad R(1) = 1$$

$$[B_{-1}]\{\Phi(-1)\} = \{0\}, \quad [B_1]\{\Phi(1)\} = \{0\}$$

This ODE system can then be solved by any general-purpose ODE package. It appears that even though the order of the new system is increased by two, it is still very advantageous in the algorithm implementation. An obvious convenience in this case is to have an easy-to-make programming format and understandable time saving procedure in preparing the problem for a standard ODE solver.

In order that the convergence of non-linear system (23), one by one, to the first N eigen-pairs can be assured and routinized, a series of initial guesses appropriate for the non-linear solution of system by a standard ODE solver should be generated. The inversion iteration is used as follows to solve linear system (24) with initial eigen-pairs adequately set for $\{\Phi\}$,

$$\{\tilde{\Phi}\}^{(k)} = [L]^{-1}[M]\{\Phi\}^{(k-1)}$$

$$\lambda^{(k)} = \frac{1}{\|\tilde{\Phi}^{(k)}\|_M}, \quad \{\Phi\}^{(k)} = \frac{\{\tilde{\Phi}\}^{(k)}}{\|\tilde{\Phi}^{(k)}\|_M}, \quad k = 1, 2, \ldots \tag{24}$$

Although an inverse iteration may be used alone to solve eigen-problem (20), the convergence is often very slow as $|\lambda_1/\lambda_2|$ is close to 1. This is why only a small number of inverse iterations are applied to generate a relatively pure eigen-function, and the components of higher-order eigen-functions are mostly filtered out or at least negligible. Once the first $i-1$ eigen-value and vector

are obtained, the preprocessing of orthogonalizing $\{\Phi\}$ must be taken to remove the components of the first $i-1$ eigen-functions from the provided trial function. With this moderately accurate eigen-solution as the initial guess, the above direct non-linear solution process can thus be used to speed up the convergence and sharpen the accuracy of the sought eigen-pairs. This strategy has been founded to be much more efficient and powerful than either pure inverse iteration or direct non-linear solution.

3. EXAMPLES AND DISCUSSION

To show the accuracy and efficiency of the proposed FEMOL scheme, three numerical examples are presented, all of which are of irregular geometry.

(A) As the first example, the cross-section of an eccentric coaxial line is described in the w-plane as shown in Figure 3(a), which is ready for a conformal mapping transformation. Radii of the inner and outer circles are R_1 and R_2, respectively. D is the distance between the two centre points of circle. A mapping procedure, characterized by $w = R_1 \sinh x_1 \coth z/2$, transforms the outer circle ABC of radius R_1 and its centre at $(R_1 \sinh x_1, 0)$ in the w-plane to a straight line $A'B'C'$ in the z-plane as illustrated in Figure 3(b). Co-ordinates of the points $A'B'C'$ are, respectively, $x_1 - j\pi, x_1 + j0$ and $x_1 + j\pi$. This conformal mapping also transforms the circle EFG of radius R_2 into the w-plane with its centre at $R_1 \cosh x_2(\sinh x_1/\sinh x_2), 0)$ to a straight line $E'F'G'$ in the z-plane. Co-ordinates of the points $E'F'G'$ are, respectively, $x_2 - j\pi$, $x_2 - j0$ and $x_2 + j\pi$. As a result, the Helmholtz equation in the w-plane can be converted into a weighted Helmholtz equation in the z-plane as follows:

$$\frac{\partial^2 u}{\partial x^2} + \frac{\partial^2 u}{\partial y^2} + k^2 R_1^2 \left\{ \frac{\sinh(x_1)}{\cosh(x) - \cos(y)} \right\}^2 u = 0 \tag{25}$$

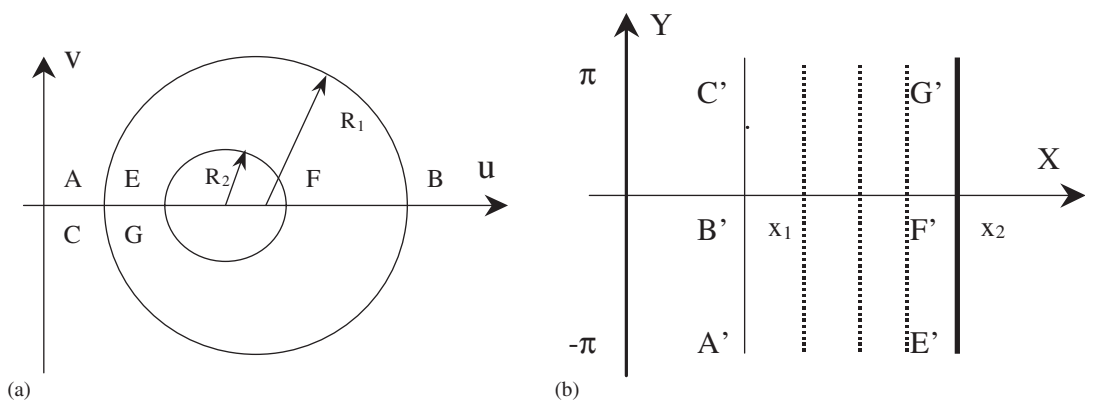

Figure 3. Geometrical representation of an eccentric coaxial line in the w-plane (original domain) and in the z-plane (transformed domain) for conformal mapping transformation. (a) w-plane representation; and (b) z-plane representation.

Table I. Comparative results of TM cutoff wave-numbers for the eccentric coaxial lines between the proposed FEMOL and finite-difference (FD) method.

		$\frac{R_2}{R_1}=\frac{2}{3}$, $\frac{D}{R_1}=0.2$		$\frac{R_2}{R_1}=\frac{1}{4}$, $\frac{D}{R_1}=0.25$	
J	Symmetry	FEMOL	FD method	FEMOL	FD method
1	S	6.226	6.217	3.457	3.446
2	A	6.894	6.887	4.253	4.248
3	S	7.657	7.650	4.904	4.897
4	A	8.353	8.347	5.498	5.488
5	S	9.023	8.990	5.872	5.862
6	A	9.674	9.610	5.569	6.552
7	S	10.315	10.309	6.587	6.580
8	A	10.941	10.932	6.621	6.626
9	S	11.537	11.523	7.453	7.460
10	A	12.417	12.423	7.506	7.513

Table II. Comparative results of TE cutoff wave-numbers for the eccentric coaxial lines between the proposed FEMOL and finite-difference (FD) method.

		$\frac{R_2}{R_1}=\frac{2}{3}$, $\frac{D}{R_1}=0.2$		$\frac{R_2}{R_1}=\frac{1}{4}$, $\frac{D}{R_1}=0.25$	
J	Symmetry	FEMOL	FD method	FEMOL	FD method
2	A	1.189	1.189	1.638	1.633
3	S	1.319	1.318	1.667	1.663
4	A	2.423	2.418	2.905	2.908
5	S	2.435	2.422	2.928	2.915
6	A	3.427	3.415	3.911	3.899
7	S	3.575	3.565	3.987	3.972
8	A	4.670	4.669	4.349	4.352
9	S	4.689	4.672	4.728	4.654
10	A	5.803	5.717	5.037	5.055

The transformed structure of Figure 3(b) has electric walls at $x = x_1$ and x_2 and magnetic walls at $y = \pm\pi$. Higher-order modes in this case always satisfy the following boundary conditions on the electric walls: $u = 0$ for TM modes, and $\partial u/\partial n = 0$ for TE modes. On the magnetic walls, the boundary conditions for these modes are different for symmetric and asymmetric cases, namely, $\partial u/\partial n = 0$ for symmetric TE modes; $u = 0$ for asymmetric TE modes; $\partial u/\partial n = 0$ for symmetric TM modes; $u = 0$ for asymmetric TM modes.

Since calculated fields are expected to exhibit quite 'wild' behaviour in y-direction while rather 'mild' in x-direction, a discretization is made in x-direction. The mesh segmentation considered for this transformed rectangular domain is simple. Numerical results obtained by the present method together with calculations of Reference [20] on the basis of a finite-difference approach for the symmetric and asymmetric TM as well as TE modes are given in Tables I and II. Comparisons are made for the first 10 modes. Observed deviation of the results between the two techniques is less than 1.0%, and this excellent agreement justifies the validity of the present model. It is also known that the weighted Helmholtz equation

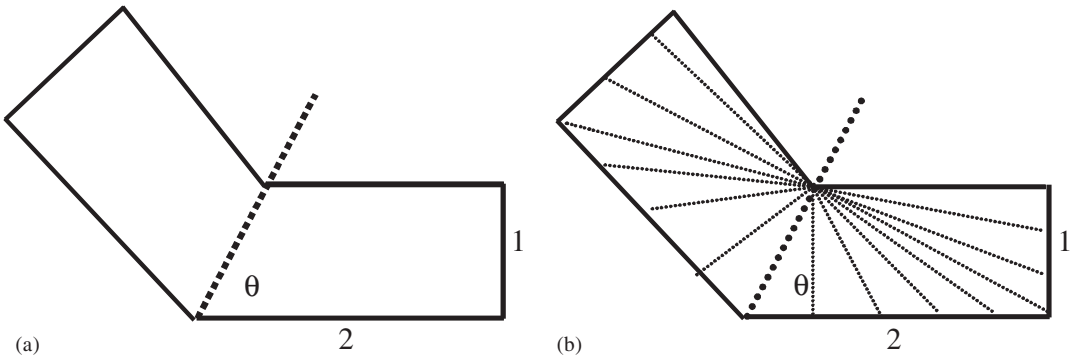

Figure 4. Cross-sectional view and proposed FEMOL mesh design for a symmetrically bending waveguide: (a) cross-section; and (b) mesh design.

Table III. Numerical results of even-ordered TM cutoff wave-numbers for the symmetric bending waveguide, calculated by the proposed FEMOL and the method of lines (MOL).

	$\theta = 30^\circ$		$\theta = 45^\circ$	
J	FEMOL	MOL method	FEMOL	MOL method
E_1^e	3.487	3.486	3.151	3.150
E_2^e	4.581	4.577	4.471	4.469
E_3^e	5.683	5.691	5.732	5.714
E_4^e	6.485	6.475	6.409	6.392

(25) could not be solved in the conventional MOL but it can easily be done by our developed FEMOL.

(B) Our second example is to calculate a bending waveguide whose cross-section is shown in Figure 4(a) and the angle ($\pi/4 \leqslant \theta \leqslant \pi/2$) denotes its bending degree. Figure 4(b) presents the mesh segmentation in dividing this irregular domain. Since the fields vary abruptly in the proximity of the corner, the discretization is selected along the circumferential direction. For this symmetrical structure, odd or even E-waves under different bending degrees are calculated by the FEMOL. This problem may be solved with the conventional MOL but much more radial lines are needed to discretize the domain in matching sharply angular boundary for higher accuracy. On the other hand, it may also be handled by the FEM but much effort is invested in mesh design and accuracy control. Calculated eigenvalues are compared in Tables III and IV between the FEMOL and conventional MOL developed in Reference [5] for two bending degrees $\theta = \pi/4$ and $\pi/2$, respectively. It can be found from our calculations that the new FEMOL (8 cubic elements) scheme requires fewer lines to match the irregular boundary as compared to the conventional MOL (50 lines) in achieving the same accuracy of solution.

(C) Our last showcase consists of an eight-sided polygon structure as described in Figure 5(a), which is known as GWW iso-spectral drum. This complex geometry is now modelled by the proposed FEMOL. The polygon, especially with re-entrant corners, has been well recognized as a numerically difficult problem. Techniques on the basis of a complete

Table IV. Numerical results of odd-ordered TM cutoff wave-numbers for the symmetric bending waveguide, calculated by the proposed FEMOL and the method of lines (MOL).

	$\theta = 30^\circ$		$\theta = 45^\circ$	
J	FEMOL	MOL method	FEMOL	MOL method
E_1^o	3.632	3.630	3.892	3.893
E_2^o	4.913	4.907	5.426	5.422
E_3^o	6.462	6.458	6.569	6.575
E_4^o	6.557	6.542	6.995	7.012

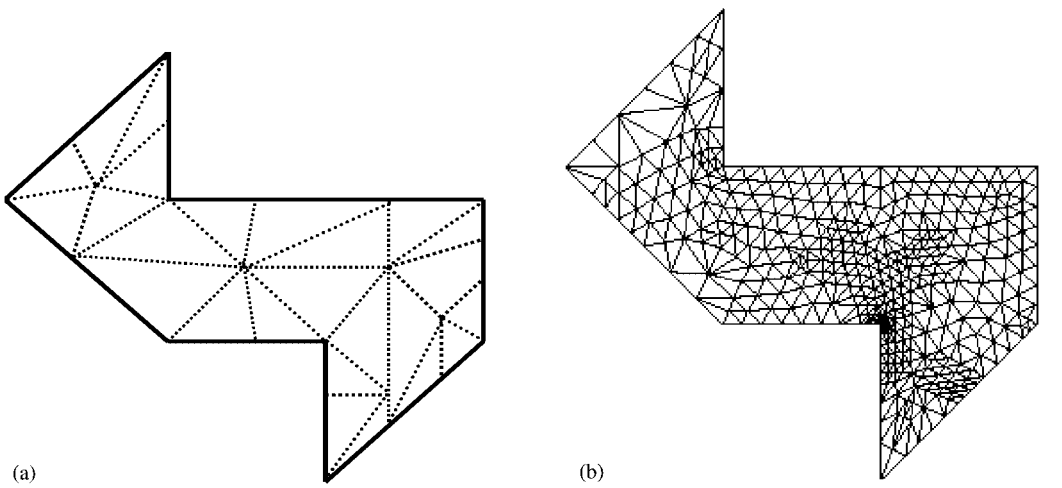

Figure 5. (a) Physical topology of a 2D eight-sided domain with complex shape. The dotted lines stand for mesh lines that partition the whole domain into a group of small segments; and (b) Adaptive mesh refinement by PLTMG for the 2D eight-sided domain.

domain discretization such as FD technique and FEM may demand an extra effort in handling singularities near the geometrical corners. Figure 5(b) shows the adaptive grid process in PLTMG for the first eigen-value on this eight-sided polygon [21]. The finest structure occurs near the corner where the eigen-value is large. At this stage, there are 966 triangles and 402 vertices and the eigen-value estimate reaches a relative accuracy of about 0.5%. The storage as well as computational time would become a serious obstacle if high accuracy is required via the FEM. The conventional MOL should use a very small mesh (line) step to match non-orthogonal boundary, which may in turn complicate its algorithm. Our proposed FEMOL cannot only match the complex boundary easily but also yield highly accurate results efficiently. A systematic comparison is shown in Table V among results obtained by the FEMOL, FD scheme [22] and measurements [23]. Although the FD method presents almost the same accuracy as the FEMOL, our technique requires a much coarser mesh scheme and it does not need any extrapolation for accurate calculations of the eigen-values as the FD method does. The Figure 6 shows the field profile for the first and higher modes in an eight-sided polygon.

Table V. Calculated and measured results for TM cutoff wave-numbers of the eight-sided polygon structure.

	FEMOL	FD method [18]	Experiment [19]
1	1.000	1.000	1.000
2	1.200	1.201	1.198
3	1.428	1.428	1.427
4	1.605	1.605	1.605
5	1.690	1.690	1.691
6	1.905	1.905	1.906
7	2.043	2.043	2.045
8	2.132	2.132	2.135
9	2.205	2.204	2.206
10	2.268	2.268	2.269

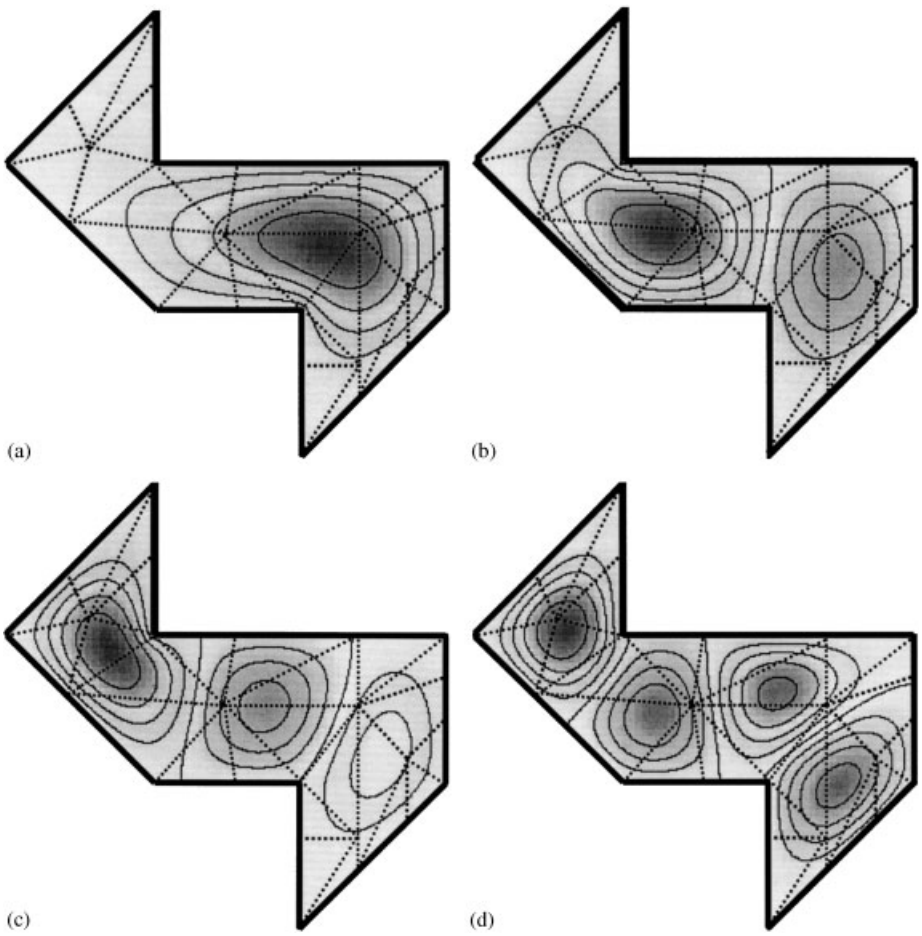

Figure 6. Field profile for the first and higher modes in an eight-sided polygon: (a) The first TM mode; (b) the second TM mode; (c) the third TM mode; and (d) the fourth TM mode.

Our above examples indicate that the developed FEMOL is able to preserve nearly all of the useful features and versatility of the FEM while enhancing the accuracy of solution and reducing a great deal of work in the mesh design and input format as required in the FE algorithm. As shown in the previous sections, the accuracy of this new technique is governed by the ODE systems characterizing the mesh line direction and by the FE interpolation along the discrete direction. To generate a reasonably accurate solution on the basis of a semi-discrete scheme, the resulting ODE system should lead to a solution with sufficient accuracy. This can be achieved by the adaptive capability in the ODE solver. The adapt is usually prone to more computational resource, which can however be compensated by avoiding a large amount of preparatory labour in mesh design and accuracy control.

4. CONCLUSIONS

In this paper, a hybrid scheme called FEMOL is introduced for efficiently solving irregular electromagnetic problems. Basic algorithmic concepts and theoretical frameworks of this new approach are described in detail through modelling and analysis of elliptical problems governed by Helmholtz equation. Results of three selected examples with arbitrary cross-sections are presented to show the efficiency and accuracy of this new method. At first glance, there seems to be nothing special here rather than the combination of two trivial techniques. In fact, our detailed description shows a number of original and interesting concepts proposed in this new scheme leading to a powerful and efficient semi-analytical numerical algorithm. In particular, the application of semi-discrete FE rather than finite difference (FD) usually implemented in the conventional MOL allows a parametric element mapping even with arbitrarily curved nodal lines and end-sides. Therefore, the FEMOL is an easy and convenient approach in dealing with a problem defined on arbitrary domain. As compared with other familiar approaches such as FEM, MOL and FD techniques, the proposed FEMOL shows a resemblance in algorithmic behaviour to the FEM and MOL but exhibits more features over its counterparts. This method can easily be extended and applied to model 3D electromagnetic field boundary value problems with complex and irregular geometry.

ACKNOWLEDGEMENTS

This work is supported partially by Natural Science Foundation of China under Contract Numbers 60271005, 60371002 and Excellent Youth Natural Science Foundation of China under Contract Number 60325103.

REFERENCES

1. Jin JM. *The Finite Element Method in Electromagnetics*. Wiley: New York, 1993.
2. Volakis JL, Chatterjee A, Kempel LC. *Finite Element Method for Electromagnetics*. The IEEE/OUP Series on Electromagnetic Wave Theory, IEEE Press: New York, 1998.
3. Shih C, Wu RB *et al*. A full analysis of microstrip lines by variational conformal mapping technique. *IEEE Transactions on Microwave Theory and Techniques* 1988; **MTT-36**:576–581.
4. Worm SB, Pregla R. Hybrid mode analysis of arbitrary shaped planar microwave structures by the method of lines. *IEEE Transactions on Microwave Theory and Techniques* 1984; **MTT-32**:191–196.

5. Chen RS, Fang DG, Li XG. Analysis of the coupling between the cylindrical microstrip lines. *Microwave and Optical Technology Letters* 1993; **6**(4):256–258.
6. Davidovitz M. Calculation of multiconductor microstrip line capacitances using the semidiscrete finite element method. *IEEE Microwave and Guided Wave Letters* 1991; **1**(1):5–7.
7. Chen RS, Yung EKN, Wu K. The generalized method of lines based on discretization technique of pseudospectral method. *Microwave and Optical Technology Letters* 1999; **20**(5):339–342.
8. Chen RS, Yung EKN, Wu K, Wang DX. Generalized method of lines for helmholz equations by using discretization technique of pseudospectral method. *IEE Proceedings on Microwaves, Antennas and Propagation* 2000; **147**(1):63–67.
9. Cheung MS *et al*. *Finite Strip Analysis of Bridge*. E&FN SPON: London, 1996.
10. Yuan S, Gao J. A new computational tool in structural analysis. *Proceedings of International Conference on EPMESC*, vol. 3, Macao, 1996; 517–526.
11. Chen RS, Yung EKN, Wu K. A novel finite element method of lines to analyze electromagnetic problems. In *IEEE Antenna Propagation Symposium Dig*., Atlanta, June 1998; 264–267.
12. Chen RS, Yung EKN, Wu K *et al*. A novel finite element method of lines to analyse electromagnetic problems. *Microwave and Optical Technology Letters* 1998; **18**(4):264–268.
13. Chen RS, Yung EKN, Wu K *et al*. Method of lines based on finite element discrete technique to analyze eigenvalues of waveguides. *International Journal of Infrared and Millimeter Waves* 1999; **20**(6):1143–1153.
14. Chen RS, Yung EKN, Chan CH, Wu K. A finite element method of lines scheme for guided wave structures. *IEEE Transactions on Antennas and Propagation* 2004; **52**(3):904–907.
15. Lentini M, Pereyra V. An adaptive finite difference solver for nonlinear two point boundary problems with mild boundary layers. *SIAM Journal on Numerical Analysis* 1977; **14**(1):91–111.
16. Deuflhard P, Pesch JJ, Rentrop P. A modified continuation method for the numerical solution of nonlinear two-point boundary value problems by shooting techniques. *Numerische Mathematik* 1976; **26**:327–343.
17. Bader G, Ascher U. A new basis implementation for a mixed order boundary value ODE solver. *SIAM Journal on Scientific and Statistical Computing* 1987; **8**(4):483–499.
18. Ascher U, Russell RD. Reformulation of boundary value problems into standard form. *SIAM Review* 1981; **23**(2):238–254.
19. Quanfeng W. Modified ODE-solver for vibration of tube-in-tube structures. *Computer Methods in Applied Mechanics and Engineering* 1996; **129**:151–156.
20. Das BN, Chakrabarty SB. Evaluation of cut-off frequencies of higher order modes in eccentric coaxial line. *IEE Proceedings on Microwaves, Antennas and Propagation* 1995; **142**(4):350–356.
21. Bank R. *PLTMG Users' Guide 7.0*: *A Software Package for Solving Elliptic Partial Differential Equations*. SIAM: Philadelphia, PA, 1994.
22. Hua W, Sprung DWL *et al*. Numerical investigation of isospectral cavities built from triangles. *Physical Review E* 1995; **51**(1):703–708.
23. Sridhar S, Kudrolli A. Experiments on not 'hearing the shape' of drums. *Physical Review Letters* 1994; **72**(14):2175–2178.

AUTHORS' BIOGRAPHIES

Ru-Shan Chen was born in Jiangsu, People's Republic of China, He received BSc degree in 1987 and MSc degree in 1990 both from the Department of Radio engineering, Southeast University and PhD from Department of Electronic Engineering, City University of Hong Kong in 2001. He joined the Department of Electrical Engineering, Nanjing University of Science and Technology (NUST), where he was a teaching assistant in 1990, and lecture later in 1992. Since September 1996, he was a visiting scholar with Department of Electronic Engineering, City University of Hong Kong, first as Research Associate, became a Senior Research Associate in July 1997 and a Research Fellow in April 1998. From June to September 1999, he was also a visiting scholar at Montreal University, Canada. In September 1999, he was promoted to be a full Professor and Associate Director of the Microwave and Communication Center in NUST and in 2001, Associate Head, Department of Communication Engineering, Nanjing University of Science and Technology. His research interests mainly include microwave/millimetre wave system, measurements, antenna, circuit and computational electromagnetics.

He even received the 1992 third-class science and technology advance prize given by the National Military Industry Department of China, the 1993 third-class science and technology advance prize given by the National Education Committee of China, the 1996 second-class science and technology advance prize

given by the National Education Committee of China, the 1999 first-class science and technology advance prize given by JiangSu Province, and the 2001 second-class science and technology advance prize. In NUST he was awarded the Excellent Honor Prize for academic achievement in 1994, 1996, 1997, 1999, 2000, 2001, 2002 and 2003, respectively. And he even taught several graduate courses including 'Microwave Integrated Circuits and Multi-Chip Modules', 'Genetic Algorithms and Neural Networks for Microwave Engineering Applications', 'Electromagnetic Field and Wave Theory', 'Computational Electromagnetics', 'Microwave Ferrite Theory and Applications' and 'Electromagnetic Compatibility'. He has authored or co-authored more than 120 papers including 76 papers in international journals.

Edward Kai-Ning YUNG was born in Hong Kong. He attended schools in Hong Kong and in the United States of America. He obtained a BSc degree with special distinction in electrical engineering from the University of Mississippi in 1972. He stayed with his alma mater and subsequently earned his MSc and PhD degrees in 1974 and 1977, respectively. After graduation, Edward worked briefly in the Electromagnetic Laboratory, University of Illinois at Urbana-Champaign. He returned to Hong Kong in 1978 and began his teaching career at the Hong Kong Polytechnic. He joined the newly established City University of Hong Kong in 1984 and was instrumental in setting up a new department. He was promoted to full professor in 1989, and in 1994, he was awarded one of the first two personal chairs in the University. He headed the Department of Electronic Engineering, the largest of its kind in Hong Kong with over 69 faculties, from 1995 to 2001. He founded the Wireless Communications Research Center in 1994 and is currently its Director.

Edward is active in research in microwave devices and antenna designs for wireless communications. He is the principal investigator of many funded projects worth tens of million dollars. He is the author of over 350 papers, including 200 in referred journals. Edward is also active in applied research, consultancy, and other types of technology transfers. He holds one patent. He is a fellow of the Chinese Institution of Electronics, the Institute of Electrical Engineers, and the Hong Kong Institution of Engineers. He is also a member of the Electromagnetics Academy. He is listed in the *Who's Who in the World* and *Who's Who in the Science and Engineering in the World.*

Ke Wu was born in Liyang, Jiangsu Province, China. He received the BSc degree (with distinction) in radio engineering from the Nanjing Institute of Technology (now Southeast University), Nanjing, China, in 1982 and the DEA and PhD degrees in optics, optoelectronics and microwave engineering (with distinction) from the Institut National Polytechnique de Grenoble (INPG) and the University of Grenoble, France, in 1984 and 1987, respectively.

Dr Wu conducted research in the Department of Electrical and Computer Engineering, University of Victoria, Canada, prior to joining the Ecole Polytechnique (Engineering School affiliated with the University of Montreal) as an Assistant Professor. He is currently Professor of Electrical Engineering at Ecole Polytechnique and Canada Research Chair in Radio-Frequency and Millimeter-Wave Engineering. Dr Wu held a visiting or guest professorship at Telecom-Paris, Paris, France and INP-Grenoble, France, the City University of Hong Kong, the Swiss Federal Institute of Technology (ETH-Zurich), Switzerland, the National University of Singapore, the University of Ulm and the Technische Universitaet Muenchen, Germany, as well as many short-term visiting professorships with other universities in the USA, Belgium, France, Italy, Japan, Germany, China and Tunisia. He holds an Honorary Visiting Professorship, and a Cheung Kong Endowed Chair Professorship (visiting) at the Southeast University, and an Honorary Professorship at the Nanjing University of Science and Technology, China. He has been the head of the FCAR Research Group of Quebec on RF and microwave electronics, the Director of the Poly-Grames Research Center, and the Founding Director of the Facility for Advanced Millimeter-wave Engineering (FAME) under the joint sponsorship of Canadian Foundation for Innovation (CFI), federal government of Canada, Quebec government and industries. He

has authored or co-authored over 380 referred papers, and also 10 book chapters. His current research interests involve hybrid/monolithic planar and non-planar integration techniques, active and passive circuits, antenna arrays, advanced field-theory-based CAD and modelling techniques, and development of low-cost RF and millimetre-wave transceivers. He is also interested in the modelling and design of microwave photonic circuits and systems.

Dr Wu is a member of the Electromagnetics Academy, the Sigma Xi Honorary Society, and the URSI. He has held positions in and has served on various international committees, including the Vice-Chair of the Technical Program Committee (TPC) for the 1997 Asia-Pacific Microwave Conference, the General Co-Chair of the 1999 and 2000 SPIE's International Symposium on Terahertz and Gigahertz Electronics and Photonics, the General Chair of 8th International Microwave and Optical Technology (ISMOT'2001), the TPC Chair of the 2003 IEEE Radio and Wireless Conference (RAWCON'2003) and the General Co-Chair of the 2004 IEEE Radio and Wireless Conference (RAWCON'2004). In particular, he is the promoter and organizer for the 2012 IEEE MTT-S International Microwave Symposium (IMS) in Montreal and will serve as its General Chair. Dr Wu has served on the Editorial or Review Boards of various technical journals, including the IEEE Transactions on Microwave Theory and Techniques, the IEEE Transactions on Antennas and Propagation and the IEEE Microwave and Wireless Components Letters. He serves on the Editorial Board of many international publications (non-IEEE) that include *Microwave and Optical Technology Letters*, *International Journal of RF and Microwave Computer-Aided Engineering* (*RFMiCAE*) and *John Wiley's* 6-*Volumes Encyclopedia of RF and Microwave Engineering*. Currently, Dr Wu is an Associate Editor of *International Journal of RF and Microwave Computer-Aided Engineering* (*RFMiCAE*). He served on the 1996 IEEE Admission and Advancement Committee, the Steering Committee for the 1997 joint IEEE Antennas and Propagation Society (AP-S)/URSI International Symposium. He has also served as a TPC member for the IEEE Microwave Theory and Techniques Society (IEEE MTT-S) International Microwave Symposium. Dr Wu was a Guest Editor of the IEEE Microwave Magazine. He was elected into the Board of Directors of the Canadian Institute for Telecommunication Research (CITR). He served on the Technical Advisory Board of Lumenon Lightwave Technology Inc. He served as a member of many government-sponsored research grants selection panels around the world. He has been a special member of the *Commission Scientifique* of the INRS in Quebec. He is the Chair of the Joint IEEE Chapter of MTTS/APS/LEOS in Montreal, and the Co-ordinator of IEEE MTT-S Region-7 Chapters.

Dr Wu was the recipient of a number of awards and prizes, which include a URSI Young Scientist Award, the IEE Oliver Lodge Premium Award, the Asia-Pacific Microwave Prize, the first University Research Award 'Prix Poly 1873 pour l'Excellence en Recherche' presented by the Ecole Polytechnique on the occasion of its 125th anniversary, and the Urgel-Archambault Prize (highest honor) in the field of physical sciences, mathematics and engineering from the French–Canadian Association for the Advancement of Science (ACFAS). In 2002, he was the first recipient of the IEEE MTT-S Outstanding Young Engineer Award. He was the recipient of the 2004 Fessenden Medal of the IEEE Canada with the citation '*for many pioneering contributions to RF*, *microwave and millimetre-wave theory and techniques*, *in particular*, *the invention of substrate integrated circuits* (*SICs*) *for future wireless systems*'. He is listed in the Who's Who directories. He is a Fellow of the IEEE, and a Fellow of the Canadian Academy of Engineering (CAE).

